machines

MDPI

Article

Streamlined Bearing Fault Detection Using Artificial Intelligence in Permanent Magnet Synchronous Motors

Javier de las Morenas [1,2,*], Lidia M. Belmonte [1,2] and Rafael Morales [2,3]

[1] Escuela Técnica Superior de Ingeniería Industrial de Albacete, Universidad de Castilla-La Mancha, 02071 Albacete, Spain
[2] Instituto de Investigación en Informática (I3A), Universidad de Castilla-La Mancha, 02071 Albacete, Spain; rafael.morales@uclm.es
[3] Escuela Técnica Superior de Ingeniería Industrial de Ciudad Real, Universidad de Castilla-La Mancha, 13071 Ciudad Real, Spain
* Correspondence: javier.delasmorenas@uclm.es

Abstract: Permanent magnet synchronous motors (PMSMs) are widely used in industrial applications due to their high efficiency and reliability. However, bearing faults remain a critical issue, necessitating robust fault detection strategies. This paper proposes an edge–fog–cloud architecture for bearing fault detection with a specific focus on implementing an efficient and non-intrusive edge-based solution. The methodology involves preprocessing motor current signals through fast Fourier transform (FFT) and Hilbert transform-based envelope analysis to extract harmonics without being masked by the fundamental supply frequency. These features are used to train machine learning models, considering variations in both speed and load. Experimental validation is conducted using the Paderborn University Bearing Dataset, demonstrating that the proposed approach achieves exceptional accuracy, precision, recall, and F1-score, exceeding 0.98 with models such as XGBoost, LightGBM, and CatBoost. While CatBoost exhibits the highest performance, LightGBM is selected as the optimal model due to its significantly reduced training time, making it well suited for edge computing applications. A comparison with prior studies confirms that the proposed method delivers competitive performance while utilizing fewer sensors, reducing hardware complexity. This research lays the groundwork for future predictive maintenance strategies ensuring real-time diagnostics and optimized industrial deployment.

Keywords: non-intrusive condition monitoring; bearing fault detection; edge–fog–cloud computing; artificial intelligence; raw data preprocessing

check for updates

Academic Editors: Davide Fonseca and Antonio J. Marques Cardoso

Received: 3 March 2025
Revised: 22 April 2025
Accepted: 24 April 2025
Published: 24 April 2025

Citation: de las Morenas, J.; Belmonte, L.M.; Morales, R. Streamlined Bearing Fault Detection Using Artificial Intelligence in Permanent Magnet Synchronous Motors. *Machines* **2025**, *13*, 357. https://doi.org/10.3390/machines13050357

Copyright: © 2025 by the authors. Licensee MDPI, Basel, Switzerland. This article is an open access article distributed under the terms and conditions of the Creative Commons Attribution (CC BY) license (https://creativecommons.org/licenses/by/4.0/).

1. Introduction

The permanent magnet synchronous motor (PMSM) has gained significant attention due to its high efficiency, power density, and wide application in industries such as electric vehicles, renewable energy, and aerospace [1,2]. However, like any electrical machine, PMSMs are susceptible to various types of faults, including stator winding failures, rotor demagnetization, bearing degradation, and eccentricity issues [1,3,4]. The early detection of these faults is crucial to ensuring system reliability, reducing downtime, and preventing catastrophic failures.

Traditionally, induction motor (IM) fault diagnosis techniques, such as motor current signature analysis (MCSA) [5–7], thermal analysis [8–10], vibration-based methods [11–13], or a combination of them [14–16], have been widely employed. However, the direct application of these methods to PMSMs presents challenges due to differences in machine topology, control strategies, and fault manifestation mechanisms.

With the advancement of artificial intelligence (AI) technologies, new possibilities have emerged for enhancing fault detection in PMSMs. AI-based approaches, particularly machine learning (ML) [17,18] and deep learning (DL) models [3], can extract meaningful patterns from operational data, enabling real-time fault detection and classification.

This paper explores how traditional IM-based fault detection techniques can be adapted and enhanced using AI methodologies for effective PMSM fault diagnosis. The proposed fault detection approach is specifically designed for industrial environments, ensuring feasibility for real-world applications without the need for sophisticated laboratory equipment. By leveraging a non-invasive methodology that requires no additional hardware installation, this solution operates with minimal hardware, making it a cost-effective and practical alternative for fault detection in industrial settings. To validate the proposed methodology, real-world bearing fault data from the Bearing Data Center of the Chair of Design and Drive Technology, Paderborn University [19], will be used for training and testing AI models. The main contributions of this paper are outlined below:

- A review of bearing fault detection methods in PMSMs and IMs with emphasis on hybrid models combining signal-based and AI-based approaches.
- Edge–fog–cloud architecture concept for fault detection, where the edge performs short-term diagnostics, the fog retrains the model, and the cloud develops a digital twin for long-term analysis and prediction.
- Implement streamlined AI fault classification at the edge using a Raspberry Pi tailored for real-world industrial environments, minimizing hardware and software requirements.
- A comparative analysis of conventional AI and deep learning AI in bearing fault detection techniques for PMSMs.

The remainder of this paper is structured as follows: Section 2 presents a review of fault detection techniques for IMs and PMSMs. Section 3 details the proposed methodological framework, integrating AI technologies. Section 4 discusses experimental results and performance evaluations. Finally, Section 5 summarizes the conclusions and future research directions.

2. Review of Fault Detection Techniques for IMs and PMSMs

The detection of faults in electric motors has been widely studied, especially in the context of IMs and PMSM [1,3,4,20], which have been the subject of extensive research due to their industrial prevalence. Various fault detection techniques have been developed, ranging from analytical methods to modern data-driven approaches.

2.1. Fault-Type Diagnostics

Fault diagnosis in PMSMs can be categorized into three main groups: electrical faults, permanent magnet-related faults, and mechanical faults [4,20]. Electrical faults typically include issues related to the stator winding insulation, phase unbalance, and inverter-related failures that disrupt normal motor operation. Faults associated with the permanent magnets (PMs) mainly involve demagnetization, magnet misalignment, or degradation due to thermal effects or mechanical stresses, leading to a loss in torque production and efficiency reduction. Mechanical faults encompass a wide range of issues, including bearing defects, rotor eccentricity, and misalignment, which can generate vibration anomalies and lead to progressive system degradation if not addressed promptly.

Effective fault detection and diagnostics in PMSMs require the integration of multiple analysis techniques, such as model-based estimations, signal processing, and artificial intelligence, to accurately classify and mitigate potential failures.

2.2. Methods

Various methodologies exist for detecting faults in rotating machinery, each with distinct advantages depending on the complexity of the system, available data, and computational resources. The three primary approaches—model-based, signal-based, and AI-based—offer complementary strategies for fault diagnosis, enhancing the reliability and efficiency of predictive maintenance systems.

The model-based approach [21,22] relies on a mathematical or physical model of the machine to predict its normal operating behavior. By comparing the theoretical response with the real-time measurements, any significant deviations may indicate potential faults. This method is particularly effective when the model is accurate and well calibrated, enabling the detection of anomalies such as unexpected torque fluctuations, deviations in rotor speed, or abnormal current variations [23]. However, its effectiveness heavily depends on the fidelity of the model, as inaccuracies or unmodeled system dynamics can lead to false alarms or undetected failures. As the complexity of the system increases, the model becomes more nonlinear [1].

In the signal-based approach, measured signals such as vibrations, currents, or voltages are analyzed directly during machine operation [3]. Advanced signal processing techniques, including Fourier transform, wavelet transform, and envelope analysis [4], are applied to extract meaningful features and identify deviations from normal behavior [20]. This approach is particularly useful for early-stage fault detection, as it can capture subtle changes in machine operation before catastrophic failure occurs. However, its main limitation lies in the requirement for domain expertise to correctly interpret signal variations and differentiate between normal fluctuations and actual faults.

The AI-based approach leverages machine learning algorithms and artificial intelligence to detect faults by recognizing patterns from historical and real-time data [20]. These models, including supervised learning classifiers such as Random Forest, XGBoost, and deep neural networks (DNN), as well as unsupervised techniques such as autoencoders and clustering, continuously learn and adapt, improving fault detection accuracy over time. Unlike traditional methods, AI-based approaches do not require explicit mathematical modeling of the system, making them highly effective in complex industrial environments where relationships between variables are difficult to model explicitly. Furthermore, deep learning methods [3] can autonomously extract relevant features from raw signals, reducing the need for extensive feature engineering. However, these models require large datasets for training, and their interpretability can sometimes be challenging [24].

Each approach has distinct advantages and limitations, making them suitable for different operational scenarios. Model-based techniques offer high interpretability but require precise modeling, while signal-based methods are effective for real-time monitoring but require expertise in feature extraction. AI-based approaches, on the other hand, excel in adaptability and automation but require substantial data for training and validation. In practice, hybrid models that combine these techniques often produce the most robust and reliable fault detection systems, leveraging the strengths of each method to improve accuracy and robustness.

2.3. Bearing Faults Detection

In electric machines, bearings play a critical role in supporting the rotor and allowing mobility between the rotor and stator while enabling axial movement, as shown in Figure 1. They minimize friction and wear between moving components, ensuring smooth and efficient rotation. Bearing fault detection is a crucial aspect of condition monitoring in rotating machinery, as bearing defects can lead to severe mechanical failures if not detected in time. Various techniques have been developed to diagnose bearing faults, utilizing

different types of measured signals, including vibration, acoustic emissions, stator currents, and temperature variations, to then train machine learning models.

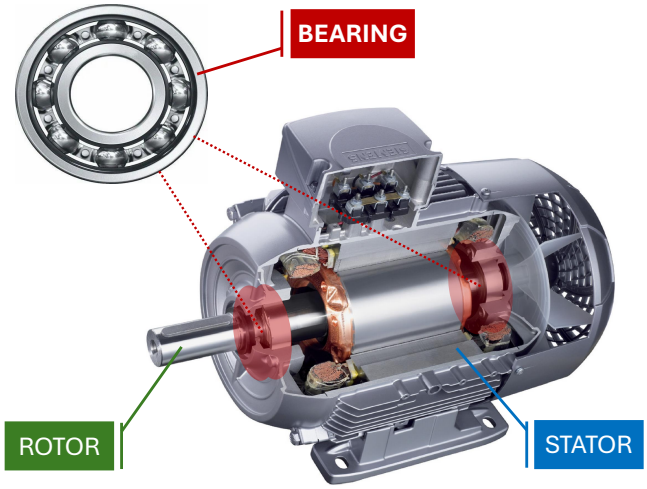


Figure 1. Bearing location in electrical machines adapted from [25].

Vibration analysis is one of the most widely used methods for bearing fault detection due to its high sensitivity to mechanical anomalies. It involves time-domain, frequency-domain, and time-frequency analysis techniques such as fast Fourier transform (FFT), envelope analysis, and wavelet transform (WT).

In [26], nine features were extracted from the vibration signals to train a model. These features included maximum, minimum, mean, standard deviation, root mean square (RMS), skewness, kurtosis, crest factor, and shape factor. The proposed fine-tuned tabNet convolutional neural network long short-term memory model demonstrated a noteworthy level of accuracy, achieving 96%. This performance surpasses that of other models, including convolutional neural network (CNN), long short-term memory (LSTM), CNN-LSTM with Gradient Boosting, and CNN-LSTM with Random Forest.

In [27], the model is trained using features extracted from vibration and acoustic signals. The proposed methods leverage time-spectral feature extraction and wavelet packet transform (WPT) for feature extraction, which are followed by classification using various machine learning classifiers such as support vector machine (SVM), RF, and linear discriminant analysis (LDA). Specifically, the method based on WPT and RF achieved an accuracy of 96.79% using acoustic signals, while the method based on time-spectral features and LDA achieved an accuracy of 98.28% using a combination of vibration and acoustic signals.

The features extracted from the vibration signals are also used in [28]. The particle swarm optimization-based continuous wavelet transform (PSO-CWT) is proposed to generate two-dimensional time–frequency spectra, and a self-adaptive feature pyramid network (SA-FPN) is proposed for feature extraction. Specifically, the PSO-CWT optimizes the center frequency and bandwidth of the wavelet function to enhance fault-related features, while the SA-FPN dynamically merges multiscale features and adjusts fusion weights based on data characteristics. The proposed method demonstrated superior performance in fault identification accuracy, particularly in complex and high-noise working environments, compared to traditional methods.

In [29], the model is trained using features extracted from vibration signals. FFT is used to preprocess the raw vibration signals into frequency-domain signals, which is followed by a two-stage methodology. In the first stage, an isolation forest module operates in an unsupervised mode to isolate operational anomalies. In the second stage, an adversarial

discriminant domain adaptation module performs in-depth fault diagnosis using a 1D CNN for feature extraction. The proposed method achieved an accuracy of 95.67% on the XJTU-SY and CWRU bearing datasets.

Vibration noise signals have also been used to train models [30]. The random-masked sliding window (RMSW) method is used to generate sub-signals, which are then converted to Mel-spectrums for feature extraction. The preprocessing of vibration signals includes applying a Mel-scale filter bank to transform the frequency to the Mel-scale, which is linear in human perception. Specifically, the RMSW-Mel-CSST model achieved an accuracy of 90.90% in classifying vibration signals.

In [31], the model is also trained using features extracted from vibration signals. The proposed methods make use of an adapted local binary pattern (ALBP) and short-time Fourier transform (STFT) for feature extraction. The preprocessing of vibration signals includes applying STFT to obtain time-frequency information and then using ALBP to generate binary patterns based on the mean intensity of selected matrices. The proposed method achieved diagnostic accuracy ranging from 99% to 99.8%, significantly outperforming traditional local binary pattern (LBP) and CNN-SVM models.

Envelope analysis is particularly effective for detecting early-stage bearing defects, as it isolates high-frequency impact signals that may be masked by fundamental rotational components.

Motor current signature analysis is another effective technique, which indirectly detects bearing faults by analyzing variations in the motor's electrical current. Bearing failures induce load fluctuations that lead to characteristic frequency components in the stator current spectrum. This approach is particularly advantageous in cases where vibration sensors are impractical, such as in hermetically sealed systems.

In [32], the model is trained using features extracted from current and speed signals. Envelope analysis and WPT are used for feature extraction, which are followed by classification using a support vector machine. The effectiveness of these methods is demonstrated through experimental measurements, showing higher detection accuracies compared to other approaches. Specifically, the method based on envelope analysis and SVM achieved an accuracy of 97.3% using the speed signal and 96.6% using the current signal, outperforming other models such as CNN and LSTM.

The features extracted from the inverter signals are used in [33]. Envelope analysis is also used for feature extraction and CNN for classification. Specifically, the study uses standard industrial inverter measurements such as phase current, stator current, rotor speed, and angular acceleration. The preprocessing of current signals includes calculating the difference between two stator phase currents $i_u = i_w - i_v$ and the stator current in rotor fixed coordinates i_s. The CNN-based approach achieved superior performance in fault identification accuracy compared to traditional methods.

Another example where the model is trained using features extracted from stator current signals is illustrated in [34]. It makes use of empirical mode decomposition (EMD), FFT, and discrete wavelet transform (DWT) for feature extraction, which are followed by classification using an attention-enhanced autoencoder-gated recurrent unit (AAGRU) model. Specifically, the preprocessing of current signals includes separating the signal into intrinsic mode functions (IMFs) using EMD, applying FFT to convert the signals to the frequency domain, and using DWT to decompose the signals into different frequency bands.

Temperature monitoring is a simpler yet less sensitive method of detecting bearing faults. As bearing degradation progresses, friction increases, leading to a rise in temperature. Although temperature-based detection is effective for identifying severe bearing damage, it is not suitable for early fault detection, as significant thermal variations occur only in advanced fault stages.

In [12], the extraction of features from thermal images is studied. They leverage statistical and gray-level co-occurrence matrix (GLCM) features for feature extraction, which were followed by classification using conventional machine learning (CML) and DL techniques. The CML approach achieved a classification accuracy of 98.29% using SVM with a radial basis function (RBF) kernel, while the DL approach using a simplified CNN achieved 100% accuracy.

The utilization of infrared thermography, in conjunction with FFT and an artificial neural network (ANN), has yielded favorable outcomes in the detection of failures in IM and gearboxes, as evidenced in [35].

Table 1 provides a summary of the literature review, which is categorized by the type of signal analyzed, the features extracted, and the model applied. All of them are a hybrid between signal-based and AI-based. It can be observed that vibration analysis methods are the most utilized due to their high sensitivity to mechanical anomalies. The listed methods demonstrate a wide range of feature extraction techniques, from statistical features (e.g., mean, RMS, kurtosis) to more complex methods such as PSO-CWT and SA-FPN. The use of advanced models such as TabNet CNN-LSTM and RMSW-Mel-CSST highlights the trend toward integrating deep learning techniques to improve fault detection accuracy. Another approach involves integrating data from multiple sources to produce more consistent, accurate and useful information, which is known as Information Fusion (IF) [36].

Table 1. Summary of fault detection methods in literature review.

Signal	Ref.	Model Used	Features Extracted
Vibration			
	[26]	TabNet CNN-LSTM	Statistical features (e.g., mean, RMS, kurtosis).
	[27]	SVM, RF, LDA	Time-spectral features, WPT features.
	[28]	PSO-CWT, SA-FPN	PSO-CWT features, SA-FPN features.
	[29]	Isolation forest, adversarial discriminant domain adaptation, 1-D CNN	FFT features.
	[30]	RMSW-Mel-CSST model	RMSW-Mel features.
	[31]	ALBP, STFT	ALBP features, STFT features.
Current			
	[32]	SVM	Envelope analysis features, WPT features.
	[33]	CNN	Envelope analysis features from inverter signals.
	[34]	AAGRU model	EMD features, FFT features, DWT features.
Temperature			
	[12]	SVM (RBF kernel), simplified CNN	Statistical and GLCM features from thermal images.
	[35]	ANN	Infrared thermography features, FFT features.

As observed in the literature review, the application of machine learning and deep learning techniques for fault detection in electrical machines is widely adopted. These approaches have demonstrated high classification accuracy and robustness in various scenarios. However, many existing solutions rely on extensive sensor networks, intrusive sensors—such as vibration and acoustic sensors—or require sophisticated laboratory equipment that may not be feasible for real-world industrial applications.

This paper aims to harness the power of machine learning while adhering to a minimal-sensor approach, utilizing only a current sensor for fault diagnosis. The selection of motor current signature analysis as the primary diagnostic tool is driven by its non-intrusive nature and its availability in virtually all industrial motor drive systems, eliminating the need for additional hardware installations.

Furthermore, the proposed methodology is designed to be practical and implementable in real-time conditions without requiring expensive laboratory setups. To achieve this, the signal processing and classification stages are optimized to run efficiently on embedded hardware, such as Raspberry Pi or similar edge computing devices. By reducing both sensor dependency and computational overhead, this paper presents a cost-effective and scalable solution for real-world deployment, ensuring that fault detection can be carried out seamlessly in industrial environments without the need for high-end measurement systems.

2.4. Approaches to the Paderborn Dataset

There are some public datasets in which machine learning methods can be tested for bearing fault diagnosis. This paper uses one of them, in concrete, the University of Paderborn dataset [19]. Although it will be properly presented in Section 4, other works using the same data are described below.

Geetha and Geethanjali [37] present a highly effective approach using a combination of vibration and motor current signals. The method involves segmenting the input signals and extracting three time-domain features: mean absolute value (MAV), simple sign integral (SSI), and waveform length (WL). These features are then classified using k-nearest neighbor (k-NN) and support vector machine (SVM) models. The proposed method achieves an impressive accuracy of 100%, demonstrating its robustness and reliability in the identification of bearing faults.

Luo et al. [38] present a novel method for fault diagnosis using a combination of vibration and motor current signals. The method involves preprocessing the current signals using Clarke transformation and wavelet packet decomposition (WPD) to improve fault-related features. The features are then aligned using synchronization-induced cross-modal contrastive learning (SICMCL) and classified using a contrastive vibration–current (CVC) framework. This approach achieves an accuracy of 99.81% with precision, recall, and F1-score values all around 99.8%. The study highlights the effectiveness of combining different signal modalities and advanced preprocessing techniques.

Li and Wang [39] describe a technique involving vibration signals in the time, frequency, and time-frequency domains for fault diagnosis. The approach involves converting vibration signals into these three domains and then applying a bilinear model and multi-head attention for fine-grained feature fusion. This method achieves a high diagnostic accuracy of 99.8%, significantly improving the performance compared to other methods. The study highlights the effectiveness of fully utilizing vibration signals from multiple domains to enhance fault diagnosis accuracy.

Nishat Toma and Kim [40] focus on diagnosing using two motor current signals. The paper employs discrete wavelet transform (DWT) for feature extraction, utilizing three types of wavelets (db4, sym4, and Haar) to decompose the current signal. The extracted features are then used to train two ensemble machine learning classifiers, Random Forest and Extreme Gradient Boosting (XGBoost). The proposed method achieves an accuracy of 99.3%. The study highlights the importance of feature extraction and the use of ensemble learning algorithms to improve classification performance.

Toma et al. [41] introduce a strategy that employs two motor current signals. The approach involves the use of discrete wavelet transform (DWT) to extract 132 statistical features from the motor current signals. These features are then optimized using a Genetic Algorithm (GA) to select the most relevant ones. The selected features are used to train a Random Forest classifier. The method achieves an accuracy of 99.7% with precision, recall, and F1-score all at 0.99. This high performance demonstrates the effectiveness of combining DWT for feature extraction and GA for feature selection.

Luo et al. [38] detail a procedure using two motor currents. This approach employs Clarke transformation and wavelet packet transform (WPT) to extract features. These features are then used in a synchronization-induced cross-modal contrastive learning framework. The method achieves an accuracy of 98.78%, with precision, recall, and F1-score all around 0.9877. This high performance demonstrates the effectiveness of combining Clarke transformation and WPT for feature extraction in diagnosing bearing faults using motor current signals.

Hoang and Kang [36] discuss a method using motor current signals. This approach involves transforming 1D signal segments into 2D square matrices (images) and then using a convolutional neural network (CNN) to automatically extract features. The extracted features are then classified using a multilayer perceptron. The method achieves an accuracy of 98.3%.

Toma et al. [41] explore a method that leverages one motor current signal. This approach involves the use of discrete wavelet transform (DWT) to extract 132 statistical features from the motor current signals. These features are then optimized using a Genetic Algorithm (GA) to select the most relevant ones. The selected features are used to train a Random Forest classifier. The method achieves an accuracy of 91.12% with precision, recall, and F1-score all at 0.91.

To facilitate a comparative analysis of previously published methods that utilize the same dataset, Table 2 has been prepared. The table shows the type and number of input signals used in each approach, how the data are preprocessed, the features used to train the model, and the classification method employed. Furthermore, the accuracy, precision, recall, and F1-score metrics from each method have been incorporated. It can be observed that advanced preprocessing techniques such as Clarke transformation, WPT, and DWT are critical to achieving high levels of accuracy. The variety of models used, ranging from k-NN to LightGBM, indicates that there is no single approach that is superior in all cases. Instead, the combination of input signals, preprocessing, and features plays a critical role in determining overall performance.

Most studies either rely on vibration signals, which necessitate the use of intrusive sensors or utilize at least two motor current signals to achieve high diagnostic accuracy. Few publications use only one current signal as input to the model. Those that do perform worse than approaches that use vibration signals or two current signals.

Table 2. Comparison of the proposed method with other approaches using the same dataset.

Ref.	Input Signal	Preprocessing	Features	Model	Accuracy
[37]	1 vibration + 2-phase motor current	Segmentation	3 time-domain features.	k-NN, SVM	1.0000
[38]	1 vibration + 2-phase motor current	Clarke transformation and WPT	Synchronization-induced cross-modal contrastive learning.	Contrastive vibration-current framework	0.9981
[39]	1 vibration	TTF	Time and frequency features.	CNN	0.9980
[40]	2-phase motor current	DWT	132 (11 statistical features of 12 wavelets).	XGBoost	0.9930
[41]	2-phase motor currents	DWT	132 (11 statistical features of 12 wavelets).	GA+RF	0.9970

Table 2. *Cont.*

Ref.	Input Signal	Preprocessing	Features	Model	Accuracy
[38]	2-phase motor currents	Clarke transformation and WPT	Synchronization-induced cross-modal contrastive learning.	Contrastive vibration-current framework	0.9878
[36]	2-phase motor currents	Transformation of 1D signal segments into 2D square matrices (images)	Unknown. Automatically through CNN.	IF+MLP	0.9830
[41]	1-phase motor current	DWT	132 (11 statistical features of 12 wavelets).	GA+RF	0.9112

3. Proposed Edge–Fog–Cloud Architecture

The proposed fault detection framework is based on a hierarchical edge–fog–cloud architecture as shown in Figure 2, which was designed to optimize computational efficiency and scalability in industrial environments. This multilayered approach enables real-time fault detection at the edge, intermediate data processing at the fog level, and long-term analysis using a digital twin in the cloud. By distributing processing tasks across different levels, the system reduces latency, minimizes network congestion, and ensures accurate and timely fault diagnoses.

The edge layer is responsible for the real-time monitoring and local processing of the current signals from the motor. A low-cost embedded device, such as a Raspberry Pi, is deployed near the machine to acquire and preprocess data from the motor current sensor. Signal processing techniques, including FFT and Hilbert envelope analysis, are applied to extract relevant features indicative of bearing faults. Once the features are computed, a lightweight AI model is executed at the edge to classify the motor condition into three categories: healthy, outer race fault (OR), and inner race fault (IR). Given the constraints of edge devices, tree-based ensemble models such as Random Forest and XGBoost are preferred because of their low computational complexity and high interoperability. The classification results are then transmitted to the fog layer via MQTT for further analysis.

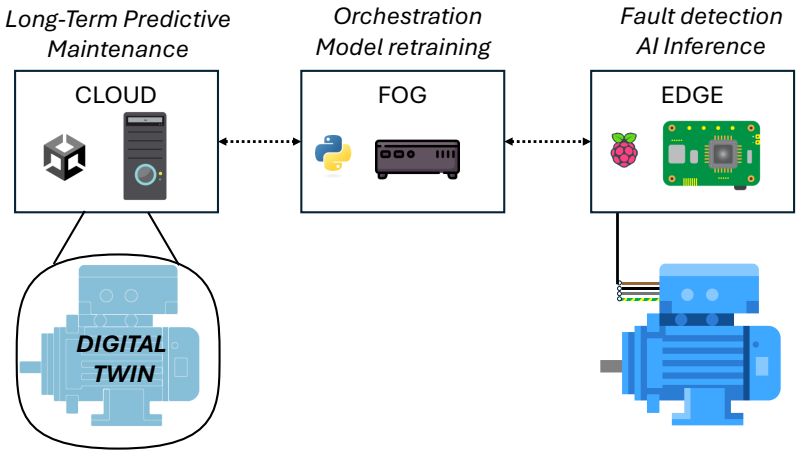


Figure 2. Proposed edge–fog–cloud architecture.

The fog layer acts as an intermediary between the edge and cloud layers, aggregating data from multiple edge devices deployed in an industrial setting. A fog computing unit, such as an industrial gateway, collects fault detection results from multiple machines, performs additional analytics to detect trends and anomalies in a fleet of motors, and

retrains the AI model with the added data to ensure it adapts to changing conditions. Subsequently, the updated model is deployed back to the edge, maintaining high accuracy and responsiveness in real-time operations.

This layer enables real-time decision support by analyzing patterns of fault occurrence and correlating them with operational parameters. Furthermore, the fog layer can dynamically adjust edge-level processing parameters, such as sampling frequency or feature extraction strategies, to optimize fault detection accuracy under varying operating conditions. If a critical fault is detected, alerts are generated and preventive actions can be recommended to maintenance personnel.

The cloud layer hosts a digital twin of the monitored PMSM system, providing a comprehensive, long-term perspective of the machine's health status. Data collected from the fog layer are used to update the digital twin, enabling advanced analytics, predictive maintenance, and failure prognosis. Environments such as Unity can support the deployment of the digital twin.

Machine learning models in the cloud are continuously refined using historical and real-time data, improving their accuracy over time. In addition, deep learning techniques, such as CNN and recurrent neural networks (RNNs), can be deployed in the cloud to analyze large-scale datasets and uncover complex fault progression patterns. The insights obtained from the cloud-based analysis are then fed back to the fog and edge layers, enhancing the overall efficiency of the fault detection system.

The proposed architecture potentially enables scalability, as additional edge devices can be seamlessly integrated into the system without overwhelming central processing units. Furthermore, by leveraging existing motor current sensors, the framework minimizes hardware installation costs while maintaining high diagnostic accuracy.

By distributing computational tasks across the edge, fog, and cloud layers, this approach balances real-time responsiveness with long-term fault prognosis, making it suitable for industrial predictive maintenance applications. In this paper, the edge layer is developed, while the fog and cloud layers are conceptual.

3.1. Minimal-Sensor Data Acquisition

To reduce the complexity of the system and improve the deployment of the system, the proposed approach prioritizes the analysis of the motor current signature over conventional vibration-based monitoring. Current sensors are already embedded in industrial motor drive systems, eliminating the need for additional hardware. This enables non-invasive fault detection while reducing installation costs and system complexity. The collected current signals are sampled at high frequency to capture bearing fault signatures, which are often characterized by harmonic components in the stator current spectrum.

3.2. Bearing Faults Harmonics

The relationship between bearing vibration and variations in the stator current spectrum can be understood by acknowledging that any changes in the air gap affect the flux density distribution. Since ball bearings support the rotor, any defects in the bearings can cause radial displacement between the rotor and the stator, leading to fluctuations in the machine's air gap. This mechanical disturbance alters the electromagnetic field, generating specific frequency components in the stator current spectrum due to rotating eccentricities occurring in both directions. These fluctuations result in characteristic fault frequencies given by [4,42,43]

$$f_{bng} = |f_s \pm m f_{i,o}| \tag{1}$$

where $m = 1, 2, 3, \ldots$, and $f_{i,o}$ represents one of the fundamental vibration frequencies associated with bearing failure, which is determined by the geometric parameters of the bearing.

$$f_{i,o} = \frac{n}{2} f_r \left[1 \pm \frac{bd}{pd} \cos \beta \right] \tag{2}$$

In this expression, n is the number of rolling elements in the bearing, f_r represents the mechanical rotor speed in Hz, bd is the diameter of the rolling elements, pd is the bearing pitch diameter, and β corresponds to the contact angle of the rolling elements.

It is important to note that according to the equation above, precise knowledge of the bearing's construction details is required to accurately compute the characteristic fault frequencies. However, for most bearings containing between six and twelve rolling elements, these characteristic frequencies can reasonably be approximated as [44–46]

$$f_i = 0.4\, n\, f_r \tag{3}$$

$$f_o = 0.6\, n\, f_r \tag{4}$$

These approximations provide a practical means of estimating characteristic bearing fault frequencies when detailed bearing specifications are not readily available.

In conventional induction motors directly connected to the power grid, the electrical frequency is fixed at 50 Hz or 60 Hz, depending on the region. However, in PMSMs, the electrical frequency is not constant but rather varies depending on the operating speed. This characteristic arises from the control methodology employed, typically via an inverter that adjusts the motor's frequency to achieve the desired rotational speed, and the phenomenon of rotor slip does not exist.

The electrical frequency of a PMSM is determined by the rotor speed and the number of pole pairs, which is given by the equation below:

$$f_s = \frac{p}{2} f_r \tag{5}$$

where f_s represents the electrical frequency of the stator current in Hertz (Hz), p denotes the number of poles and f_r is the mechanical rotor speed in Hertz (Hz). The mechanical rotor speed can be calculated from the rotational speed in revolutions per minute (RPM) using the formula $f_r = \frac{\text{RPM}}{60}$.

This frequency varies proportionally with changes in rotational speed, making frequency-based fault analysis more complex compared to fixed-frequency induction motors.

In fault analysis, the presence of characteristic fault frequencies (f_o, f_i) due to rolling bearing defects is often examined within the current spectrum. Because the electrical frequency of PMSMs is not fixed, conventional approaches based on static frequency bands are inadequate. Instead, spectral analysis must be performed in relative terms where frequencies are normalized with respect to the rotor speed.

3.3. Edge-Based Preprocessing and Feature Extraction

Real-time data processing is performed at the edge using a Raspberry Pi or an embedded computing unit, ensuring rapid fault detection without overwhelming cloud infrastructure.

To preprocess the acquired motor current signals, two key signal processing techniques are employed: the FFT and Hilbert transform-based envelope analysis. These methods enable the extraction of informative features that characterize bearing faults.

The fast Fourier transform is applied to convert the time-domain signal into the frequency domain, revealing spectral components that may indicate bearing faults. Mathe-

matically, the discrete Fourier transform (DFT) of a discrete signal $x(n)$ with N samples is defined as

$$X(k) = \sum_{n=0}^{N-1} x(n) e^{-j2\pi kn/N}, \quad k = 0, 1, \ldots, N-1. \tag{6}$$

To efficiently compute the DFT, the FFT algorithm is utilized, reducing the computational complexity from $O(N^2)$ to $O(N \log N)$. This spectral transformation enables the identification of fault-induced frequency components in the motor current signal.

To enhance fault detection, Hilbert transform-based envelope analysis is employed. The Hilbert transform $H[x(t)]$ of a signal $x(t)$ is defined as

$$H[x(t)] = \frac{1}{\pi} \int_{-\infty}^{\infty} \frac{x(\tau)}{t-\tau} d\tau. \tag{7}$$

This transformation introduces a 90-degree phase shift to all frequency components of the signal, allowing the construction of the analytic signal $x_a(t)$, which is given below:

$$x_a(t) = x(t) + jH[x(t)] = A(t)e^{j\phi(t)}, \tag{8}$$

where $A(t)$ is the instantaneous amplitude (also known as the envelope), and $\phi(t)$ is the instantaneous phase. The envelope function $A(t)$, which highlights fault-induced modulations, is computed as shown below:

$$A(t) = \sqrt{x(t)^2 + H[x(t)]^2}. \tag{9}$$

Applying the fast Fourier transform to the extracted envelope enables further spectral analysis, revealing frequency components associated with bearing defects. This methodology enhances fault diagnosis by mitigating the masking effects of the fundamental motor supply frequency, thereby improving sensitivity to fault-induced modulations.

Once the signals are processed, feature extraction is performed to obtain meaningful parameters that can train machine learning and deep learning models. The preprocessing pipeline includes normalization using the StandardScaler method to standardize feature distributions. The extracted features can be categorized into two main groups.

The frequency–domain features, derived from FFT analysis, provide statistical descriptors that quantify deviations from normal operation. These include Root Mean Square (RMS), which measures the signal's energy, Shape Factor (SF), defined as the ratio of RMS to the mean absolute amplitude, Line Integral (LI), obtained through numerical integration of the amplitude spectrum, Skewness, which evaluates signal asymmetry, and Kurtosis, which assesses the presence of sharp peaks in the spectral distribution.

The envelope features, extracted through Hilbert transform-based analysis, enhance the detectability of fault-induced modulations. The envelope spectrum is analyzed using FFT, isolating frequency components associated with bearing defects. The first four harmonics in each band are extracted based on Equations (3) and (4). These harmonic bands are proportional to the motor speed. The motor speed is calculated indirectly by knowing the fundamental frequency using FFT. Thus, it is defined in proportion to the fundamental frequency, ensuring adaptability to variations in motor speed. The process involves computing the FFT of the original current signal, identifying spectral regions where fault harmonics may occur, and dynamically adjusting the frequency bands based on the motor's operational speed.

This combined approach ensures robust feature extraction by leveraging both spectral and envelope-based information. The statistical representation of frequency-domain fea-

tures, along with enhanced visibility of fault-induced modulations from envelope analysis, facilitates improved classification accuracy and fault detection in PMSMs.

In the analysis of electrical signals from PMSMs, the amplitude of spectral components can be significantly influenced by the applied load. To ensure that the fault detection methodology remains independent of variations in load conditions, a normalization of amplitude values is necessary. In this paper, the amplitude of each spectral component is normalized using the RMS value of the current signal within each segmented window. This approach helps mitigate the influence of load variations while preserving the fault-related spectral features.

The extracted feature set is subsequently used for classification while ensuring computational efficiency at the edge. The sequence of events is shown in Figure 3.

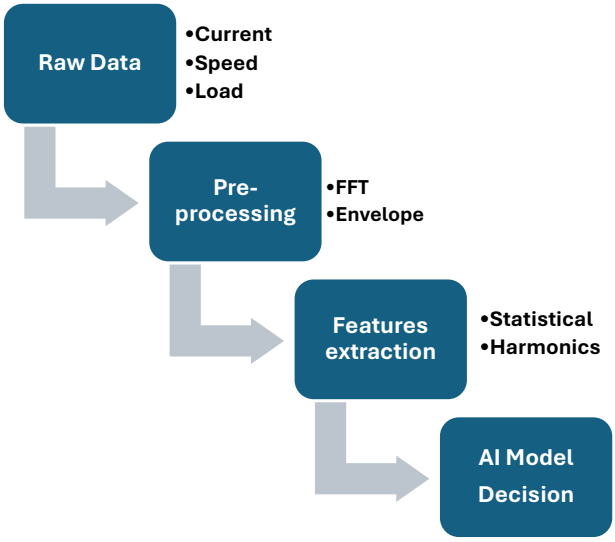


Figure 3. Edge preprocessing flowchart.

3.4. Machine Learning-Based Fault Classification

A hybrid AI approach and signal-based is employed to classify motor conditions into three categories: healthy, outer race fault (OR), and inner race fault (IR). A combination of tree-based ensemble learning methods (Random Forest, XGBoost, LightGBM, and CatBoost) and deep learning (multilayer perceptron, MLP) is used to evaluate classification accuracy.

Tree-based models are chosen due to their interpretability and low computational footprint, which make them ideal for edge deployment. They derive their name from their tree-like structure, which is used to make decisions and predictions. The structure of a tree-based model consists of nodes and branches. Each node represents a decision point based on a feature (or attribute) of the data, and each branch represents the outcome of that decision. The tree starts with a root node at the top, which then splits into branches based on certain conditions, leading to child nodes. This process continues until it reaches the leaf nodes, which represent the final predictions or outcomes [47]. Tree-based models are often considered "black-box" models during training. This means that the internal workings and the exact decision-making process can be difficult to interpret due to the complexity and the number of trees involved.

Incorporating explainability into machine learning models is particularly important in safety-critical industries, where the "black-box" nature of many advanced algorithms can hinder trust and adoption. For instance, in sectors such as healthcare, aviation and industrial automation, stakeholders need to understand and trust the decisions made by AI systems to ensure safety and compliance. As highlighted in a recent study, the development

of explainable AI models is crucial for making AI decisions interpretable by stakeholders, thereby fostering trust and facilitating the adoption of AI in safety-critical applications [48].

By making the decision-making process transparent, explainable AI helps bridge the gap between complex model predictions and human understanding. This transparency is essential for validating model behavior, ensuring regulatory compliance, and building confidence among users who rely on these systems for critical operations [49].

Despite their black-box nature during training, tree-based models can be highly explainable during inference. This is because the decision-making process can be broken down into a series of simple "if–else" rules. Tree-based models like Random Forests and Boosted Trees are more complex than single decision trees because they combine multiple trees to improve predictive performance and robustness.

Random Forests [50] work by creating an ensemble of decision trees, which are each trained on a random subset of the data and features. This randomness helps to reduce overfitting and improve generalization. During inference, each tree in the forest makes a prediction, and the final result is determined by averaging the predictions.

Boosted Trees [51–53], on the other hand, build trees sequentially, where each new tree is trained to correct the errors made by the previous trees. This process is known as boosting. The idea is to focus more on the difficult cases that previous trees misclassified. By combining the strengths of multiple weak learners (shallow trees), the boosted model can achieve high accuracy and performance. The final prediction is a weighted sum of the predictions from all the trees with more weight given to trees that perform better. The classifiers are trained using optimized hyperparameters obtained by Bayesian optimization.

The MLP model [54] is a neural network model designed to learn complex decision boundaries from extracted features. It consists of fully connected layers with dropout regularization to prevent overfitting. The Adam optimizer with an adaptive learning rate is used to improve convergence. Table 3 summarizes the characteristics of the selected models along with references for further study.

Table 3. Summary of machine learning models used for fault detection.

Model	Description
Random Forest [50]	An ensemble learning method that constructs multiple decision trees and averages their predictions to improve accuracy and reduce overfitting.
XGBoost [51]	An optimized Gradient Boosting framework that iteratively improves decision trees by minimizing errors, which is commonly used for structured data classification tasks.
LightGBM [52]	A Gradient Boosting framework designed for efficiency and scalability, using histogram-based learning for faster training.
CatBoost [53]	A Gradient Boosting model optimized for categorical data handling and fast training while reducing overfitting.
MLP [54]	A deep learning approach using fully connected neural networks with multiple hidden layers, capturing complex patterns in data.

K-fold cross-validation and Bayesian optimization ensure robustness and avoid overfitting; a stratified K-fold cross-validation approach with five folds is applied, maintaining class distribution across training and validation sets. Model hyperparameters are optimized using Bayesian search to systematically explore the parameter space while minimizing computational costs.

4. Test Case and Performance Analysis

This section presents the experimental results obtained by applying the proposed methodology to a public dataset, focusing on the edge layer. The performance of different classification models is analyzed based on key evaluation metrics.

4.1. Experimental Setup and Dataset Description

The dataset used in this paper originates from the Bearing Data Center of the Chair of Design and Drive Technology at Paderborn University [19]. It contains recordings of current, vibration, and mechanical parameters measured on a PMSM under different operating conditions. The motor under study is a Type SD4CDu8S-009 from Hanning Elektro-Werke GmbH & Co. KG (Oerlinghausen, Germany) with the characteristics presented in Table 4. It is operated by a frequency inverter (KEB Combivert 07F5E 1D-2B0A inverter, manufactured by KEB Automation KG, located in Barntrup, Germany) with a switching frequency of 16 kHz.

Table 4. Specifications of the PMSM under study.

Parameter	Value
Rated power	425 W
Nominal torque (T)	1.35 Nm
Nominal speed (n)	3000 rpm
Nominal current (I)	2.3 A
Pole pairs (p)	4

The dataset is structured to facilitate fault detection and classification tasks with a particular focus on bearing defects.

The motor was operated under four different load and speed conditions (presented in Table 5) in 32 different bearing experiments with 20 test runs per setup.

Table 5. Experimental settings.

Rotational Speed [rpm]	Load Torque [Nm]	Radial Force [N]	Name of Setting
1500	0.7	1000	N15_M07_F10
900	0.7	1000	N09_M07_F10
1500	0.1	1000	N15_M01_F10
1500	0.7	400	N15_M07_F04

The data were collected over a duration of 4 s per test, ensuring a comprehensive recording of system behavior. The sampling frequencies used for different signals are presented in Table 6.

Table 6. Sampling frequencies and number of samples per test for different signals.

Signal	Sampling Frequency	Samples per Test
Motor current	64 kHz	256,001
Vibration signals	64 kHz	256,001
Load force, load torque, speed	4 kHz	16,001
Temperature	1 Hz	240

The dataset includes three conditions: healthy condition, which represents normal operation without any detected faults; artificially damaged bearings; and bearings with real damages caused by accelerated lifetime tests.

The damage bearings include both artificially induced faults and real faults generated through accelerated lifetime testing. The artificial faults considered in this dataset include damage induced by electrical discharge machining (EDM), electric engraving, and mechanical drilling. On the other hand, real faults encompass fatigue defects, pitting, indentations due to plastic deformations, and distributed damage in both the inner ring and the outer ring, appearing in both individual and combined configurations.

This industrial-grade inverter is used to provide realistic operating conditions similar to those found in production environments. However, its presence introduces two key effects on the motor's electrical frequency characteristics:

- The electrical frequency f_s varies dynamically with the rotor speed, requiring normalization techniques in spectral analysis.
- The pulse width modulation (PWM) introduces additional spectral components at multiples of the switching frequency (e.g., 16 kHz, 32 kHz, etc.), which must be filtered to avoid misinterpretation of fault signatures.

Given these conditions, fault detection methodologies must adapt to consider the dynamic behavior of f_s, the effects of PWM harmonics, and the need for proper spectral normalization techniques.

4.2. Dataset Preprocessing

Prior to training the machine learning models, the dataset underwent several preprocessing steps to improve feature quality and ensure robustness in fault detection. The dataset consists of multiple time-domain features derived from motor current signals with measurements taken under different operational conditions.

The raw current signal was acquired at a sampling frequency of 64 kHz. The signal was segmented into windows of 1 s with a 50% overlap to improve the robustness of spectral analysis.

We conducted a standard frequency-domain analysis using the FFT. This initial approach aimed to identify prominent frequency components associated with potential mechanical faults in the permanent magnet synchronous motor. The discrete Fourier transform (DFT) was computed using the FFT algorithm, considering only the positive frequency spectrum. While this approach provided insight into the spectral content of the signal, it exhibited limitations in detecting fault-induced modulations due to the dominance of the fundamental electrical frequency. The presence of high-amplitude components in the spectrum often masked low-energy fault signatures, making them difficult to distinguish. To address these limitations, we adopted the envelope analysis technique, which allows for improved fault detection by isolating amplitude modulations associated with mechanical defects.

4.3. Feature Extraction and Selection

After computing the FFT and the envelope for each 1-second test window, the features listed in Table 7 were extracted. In total, 13 features were used along with the bearing condition label: 0 for healthy, 1 for an outer race fault, and 2 for an inner race fault. The harmonic bands correspond to those defined in Equations (3) and (4). The amplitude of the harmonic in each band is determined as the maximum value of the enveloped signal, which is normalized by the RMS of the FFT. Specifically, for the case labeled `N15_M07_F04_K001`, where the motor operates at 1500 RPM, the supply frequency is 100 Hz and the first harmonic band of the inner race fault falls within the range of 20 to 180 Hz. This highlights the necessity of using the envelope analysis to mitigate the masking effect of the fundamental frequency on the harmonics. The dataset was constructed using measurements from K001 and K002 (healthy), KA04 and KA22 (OR fault), and KI16 and

KI18 (IR fault), resulting in a total of 3351 cases, which were evenly balanced among the three classes.

The features used for the training and testing of the model are enumerated in Section 3.3 and illustrated in Table 7.

Table 7. Features used for model training.

Feature Calculation	Feature	Description
FFT-Based		
	RMS	Root mean square of the signal
	LI	Line integral of the frequency spectrum
	SF	Shape factor of the signal
	Skewness	Measure of signal asymmetry
	Kurtosis	Measure of peak sharpness in the signal
Envelope-Based		
	Harmonics 1 to 4 of Band I	Harmonic bands related to inner race fault
	Harmonics 1 to 4 of Band O	Harmonic bands related to outer race fault

4.4. Selection of Machine Learning Models

To ensure a robust classification of bearing faults in PMSMs, this paper employs a combination of tree-based ensemble methods and deep learning models. The selected models include Random Forest, XGBoost, LightGBM, CatBoost, and a multilayer perceptron neural network. Each model was chosen for its ability to handle structured data, interpretability, and classification performance.

Random Forest served as the baseline model, providing a reference for evaluating the improvements introduced by more advanced Gradient Boosting techniques such as XGBoost, LightGBM, and CatBoost. These ensemble methods were selected for their capacity to capture complex patterns and improve prediction accuracy through boosting techniques. Additionally, the MLP model was incorporated to leverage deep learning capabilities for feature extraction and representation learning, particularly in handling nonlinear relationships within the data.

4.5. Hyperparameter Optimization

The effectiveness of machine learning models heavily depends on the selection of optimal hyperparameters, which govern their learning behavior and generalization capabilities. Several hyperparameter tuning techniques exist to systematically explore the hyperparameter space, aiming to improve accuracy, robustness, and computational efficiency. This section discusses widely used approaches, including grid search, random search, Bayesian optimization, and adaptive learning rate strategies for deep learning models.

Grid search systematically evaluates all possible hyperparameter combinations within a predefined set [55]. Although this method guarantees an optimal configuration within the search space, it is computationally expensive, making it suitable only when dealing with a limited number of hyperparameters.

Random search improves efficiency by randomly sampling hyperparameter values from a predefined range [56]. Although it does not guarantee finding the absolute best configuration, empirical studies suggest that it can identify near-optimal solutions with fewer evaluations, making it practical for high-dimensional search spaces.

Bayesian optimization provides a more sophisticated approach by modeling the performance of the learning algorithm as a probabilistic function [57]. It uses prior evaluations to focus on promising regions of the hyperparameter space, reducing the number of

evaluations required for optimization. This method is particularly effective for models with complex interactions between hyperparameters, such as ensemble learning and deep neural networks.

For deep learning models, adaptive learning rate optimization further enhances performance. Techniques such as adaptive moment estimation (Adam), root mean square propagation (RMSProp), and stochastic gradient descent with momentum dynamically adjust the learning rate to improve convergence and stability. Learning rate scheduling strategies, such as ReduceLROnPlateau, further refine this process by adjusting the learning rate based on validation loss trends.

In this paper, Bayesian optimization was employed as the primary method for hyperparameter tuning due to its efficiency in exploring the search space while maintaining computational feasibility. This approach was applied to Random Forest, XGBoost, LightGBM, CatBoost, and the MLP model. For MLP, Bayesian optimization was used to tune the network architecture, dropout rate, and learning rate, ensuring an optimal configuration for classification performance. All optimizations were performed using cross-validation to improve robustness and reliability across multiple sets of data.

By implementing these optimization strategies, machine learning models achieved high predictive performance while minimizing overfitting and computational costs. The impact of these optimizations on the classification accuracy and computational efficiency is further analyzed in the subsequent sections.

Table 8 presents the optimized hyperparameters obtained for each model along with their respective training times. The execution time reflects the total duration required for model training and hyperparameter tuning. In particular, tree-based models such as Random Forest, XGBoost, LightGBM, and CatBoost exhibit varying computational demands with CatBoost requiring significantly more time due to its iterative boosting approach. MLP also demonstrates considerable optimization time, which is primarily due to the complexity of training deep neural networks. This analysis provides insight into the trade-offs between computational cost and classification performance, which are critical for real-time industrial applications.

Table 8. Optimized hyperparameters and execution time for each model.

Model	Optimized Hyperparameters	Training Time (s)
Random Forest	max_depth = 50 min_samples_split = 2 n_estimators = 150	247.79
XGBoost	learning_rate = 0.2819 max_depth = 5 n_estimators = 993	207.15
LightGBM	learning_rate = 0.2456 max_depth = 10 n_estimators = 163 num_leaves = 150	300.75
CatBoost	depth = 12 iterations = 1000 learning_rate = 0.2999	7385.51
MLP	num_layers = 2 num_units = 448 dropout_rate = 0.2019 learning_rate = 0.0030	2832.35

4.6. Performance Metrics

Evaluating the performance of machine learning models requires the use of robust and informative metrics that provide insight into classification accuracy, model reliability, and generalization performance. In this paper, multiple baseline performance metrics were used to assess the effectiveness of the selected models. These metrics include accuracy, precision, recall, and F1-score.

Accuracy is a fundamental metric that measures the proportion of correctly classified instances over the total dataset. It is calculated as

$$\text{Accuracy} = \frac{TP + TN}{TP + TN + FP + FN} \tag{10}$$

where TP represents true positives, TN true negatives, FP false positives, and FN false negatives.

Precision evaluates the proportion of correctly predicted positive instances relative to all predicted positive instances. It is given by

$$\text{Precision} = \frac{TP}{TP + FP} \tag{11}$$

This metric is particularly important in applications where false positives are costly, as it measures the reliability of positive classifications.

Recall measures the proportion of correctly identified positive instances relative to all actual positive instances. It is defined as

$$\text{Recall} = \frac{TP}{TP + FN} \tag{12}$$

A high recall ensures that most positive cases are identified, which is critical in fault detection scenarios where missing a faulty instance could have significant consequences.

F1-score is the harmonic mean of precision and recall, providing a balanced evaluation of a model's classification performance. It is computed as

$$\text{F1-score} = 2 \times \frac{\text{Precision} \times \text{Recall}}{\text{Precision} + \text{Recall}} \tag{13}$$

This metric is especially useful when there is an uneven class distribution, as it ensures both false positives and false negatives are considered.

4.7. Results

Instead of employing a fixed training and testing split, this paper used stratified K-Fold cross-validation with five folds. This approach ensures that each sample is utilized for both training and validation at different stages, thereby enhancing the model's generalization capability. In each iteration, the dataset is divided into five subsets of equal size, where four subsets are used for training and the remaining one is reserved for validation. The process is repeated five times, ensuring that every subset is used as validation data once. An independent test set was not used, firstly because of the moderate size of the dataset (3351 samples), and secondly following the standard practice observed in related work on this dataset. This choice enables a fair and direct comparison with prior studies and allows for a more comprehensive performance evaluation while mitigating biases from a single data split.

The entire machine learning pipeline is implemented using Python v3.10.12 with `scikit-learn v1.2.2`, `XGBoost v2.0.3`, `LightGBM v4.5.0`, `CatBoost v1.2.7`, and `TensorFlow 2.17.1` libraries.

The results of the cross-validation performance for the evaluated models are presented in Table 9. The table summarizes the mean accuracy along with its standard deviation as well as the precision, recall, and F1-score obtained for each classifier.

All models exhibit high classification performance with CatBoost achieving the highest cross-validation mean accuracy of 0.9830 ± 0.0052. XGBoost and LightGBM also yield strong results, demonstrating accuracies above 0.98. The MLP, while slightly lower in performance compared to tree-based models, still achieves competitive results with a mean accuracy of 0.9627 ± 0.0136. These findings confirm the robustness and effectiveness of the proposed approach for bearing fault detection using a minimal sensor setup.

The low standard deviation across the folds further indicates that the models are stable and generalize well to different data splits, reinforcing their reliability for real-world deployment in edge computing environments. These results are consistent under variable loads or speeds.

Table 9. Cross-validation performance metrics for the evaluated models.

Model	Accuracy	Precision	Recall	F1-Score
Random Forest	0.9749 ± 0.0067	0.9750 ± 0.0067	0.9749 ± 0.0067	0.9749 ± 0.0067
XGBoost	0.9803 ± 0.0065	0.9804 ± 0.0065	0.9803 ± 0.0065	0.9803 ± 0.0065
LightGBM	0.9806 ± 0.0062	0.9806 ± 0.0062	0.9806 ± 0.0062	0.9806 ± 0.0062
CatBoost	0.9830 ± 0.0052	0.9831 ± 0.0053	0.9830 ± 0.0052	0.9830 ± 0.0052
MLP	0.9627 ± 0.0136	0.9628 ± 0.0137	0.9627 ± 0.0137	0.9627 ± 0.0136

LightGBM was selected as the final model based on its superior cross-validation performance along with high precision, recall, and F1-score. This model demonstrated a favorable trade-off between computational efficiency and classification accuracy, making it well suited for real-time fault detection in edge computing environments for deployment in industrial applications.

Table 10 presents a comparison between the results presented in this paper and previous studies using the same dataset. It can be seen how the proposed method, which only requires measuring the current of one phase of a three-phase motor, achieves similar results to those using measurements from two phases of the motor current or vibration signals, which also require the installation of intrusive sensors. In practice, the use of single-phase current offers a much simpler and more cost-effective solution than approaches based on vibration sensors or multiphase current sensing. Vibration-based methods, while highly effective, require physical sensor mounting on the motor, proper installation conditions, and higher hardware and maintenance costs. On the other hand, methods based on two-phase current sensing involve more complex data acquisition systems and synchronization requirements. In contrast, the proposed single-phase approach allows for easy integration into existing systems without physical intervention on the motor or modifications to the wiring. The proposed current-based method ensures a streamlined and non-invasive solution suitable for industrial applications.

Table 10. Comparison of results between the proposed method with other approaches using the same dataset.

Ref.	Input Signal	Accuracy	Precision	Recall	F1-Score
[37]	1 vibration + 2-phase motor current	1.0000	–	–	–
[38]	1 vibration + 2-phase motor current	0.9981	0.9982	0.9980	0.9980
[39]	1 vibration	0.9980	–	–	–
[40]	2-phase motor current	0.9930	0.9900	0.9900	0.9900

Table 10. *Cont.*

Ref.	Input Signal	Accuracy	Precision	Recall	F1-Score
[41]	2-phase motor currents	0.9970	0.9900	0.9900	0.9900
[38]	2-phase motor currents	0.9878	0.9880	0.9875	0.9877
[36]	2-phase motor currents	0.9830	–	–	–
[41]	1-phase motor current	0.9112	0.9100	0.9100	0.9100
This work	**1-phase motor current**	**0.9806**	**0.9806**	**0.9806**	**0.9806**

4.8. Edge Deployment

The trained LightGBM model was deployed on a Raspberry Pi 3 Model B, which features a Broadcom BCM2837 1.2 GHz quad-core ARM Cortex-A53 processor and 1 GB of LPDDR2 RAM, using Python-based libraries for execution. This setup enabled direct model inference without requiring additional hardware acceleration or specialized inference engines. According to the flowchart or the edge layer shown in Figure 3, two main computational tasks are completed at this layer: preprocessing and feature extraction, and model inference. Several tests have been performed, achieving a performance of 28.13 ms ± 0.47 ms in preprocessing and feature extraction and an average inference time of 23.00 ms ± 1.52 ms. The system requires acquiring data for 1 s windows, and the inference execution takes 51 ms. Therefore, the total time for each cycle is approximately 1.051 s. Given this setup, fault detection can be realistically performed in 3-s intervals. These results suggest the feasibility of deploying this method for edge computing applications, highlighting its suitability for real-time execution on resource-constrained embedded systems.

In case of use external current probes to fully exploit the edge layer, it is necessary to use an MCP3008 or, similarly, a 10-bit resolution analog-to-digital converter (ADC) that communicates with the serial peripheral interface (SPI) protocol. Given the capabilities of the ADC, it is possible to achieve a sampling frequency of 4 kHz, which is a frequency eight times greater than the higher harmonic used in the inference.

In addition, the inference model was tested on an Arduino Mega. However, direct application was not feasible. It was necessary to use the m2cgen library to convert the model into C code. This model generated over 65,000 lines of code, exceeding the program memory (256 KB) of the microcontroller, reaching 233% of its capacity. Therefore, at least an ESP32 (4 MB) is required for implementation. Raspberry Pi and analogous hardware are well suited for this application.

5. Conclusions

In this paper, an edge–fog–cloud architecture is proposed for bearing fault detection in PMSM motors with a particular emphasis on the development of the edge layer. The design emphasizes non-intrusiveness, eliminates the necessity for high-performance laboratory equipment, and ensures applicability in industrial environments.

A raw data processing pipeline has been defined to extract features for training machine learning and deep learning models. This process leverages FFT and envelope analysis using the Hilbert transform, allowing the extraction of harmonics without being masked by the fundamental supply frequency. Moreover, the fundamental frequency itself is utilized to estimate motor speed, which in turn determines the frequency bands where fault-related harmonics may appear. These extracted features serve as the input for the classification models. The analysis encompasses not only the consideration of variable speed but also that of load variation.

The proposed approach has yielded exceptional outcomes, with an accuracy rate surpassing 0.98, as evidenced by the utilization of three distinct models: XGBoost, LightGBM,

and CatBoost. While CatBoost exhibited the most optimal performance, LightGBM was ultimately selected as the definitive model due to its substantially reduced training time, thereby ensuring a judiciously balanced solution for edge computing applications.

A comparison of the results with those of previous studies that used the same dataset was undertaken, the purpose of which was to demonstrate that similar performance could be achieved despite the use of a smaller number of sensors. This finding serves to validate the effectiveness of the proposed approach in reducing hardware requirements while maintaining high classification accuracy and constrained resources. The high classification accuracy coupled with low computational requirements, as presented in the implementation on a Raspberry Pi 3, demonstrates the potential of this approach for use in resource-constrained environments, paving the way for practical and scalable condition monitoring solutions.

While this study has successfully demonstrated the potential of our proposal for bearing fault detection in synchronous machines, certain limitations should be noted. Before performing the diagnosis of a PMSM, it is necessary to correctly identify the motor, since the feature extraction of the harmonics in the current directly depends on the number of poles of the motor; therefore, the preprocessing must be adapted to this characteristic before inferencing the model. The results are limited to the conditions of the dataset used with varying loads in the range of 0.1–0.7 Nm, radial forces from 400 to 1000 N, and speed from 900 to 1500 under constant conditions; further validation with additional datasets under broader conditions and real-world scenarios would support the robustness of the results presented in this work. Additionally, while we have presented performance results on a Raspberry Pi 3, the full conceptual architecture (cloud-fog-edge) was not implemented, and inter-layer latencies were not tested. The full conceptual architecture might be tested with multiple edge nodes in real industrial environments to cover and diagnose every electric motor on the shop floor with the goal of achieving zero downtime. This approach will help validate the scalability and effectiveness of the system in practical applications, ensuring its robustness and adaptability in different operational environments.

The architecture that has been presented provides a foundation for the development of future predictive maintenance strategies that will be based on cloud-executed digital twins. These models will continuously be updated with real-time data from the edge through the fog layer, where the orchestration of efficient information flow will take place. Future work will focus on the development of the fog and cloud layers of this architecture as well as on the incorporation of the detection of additional fault types to further enhance the system's capabilities. In addition, efforts will be directed toward the use of additional datasets that include variable operating conditions to further validate the robustness of the proposed methodology, and toward the implementation of the edge layer in a real industrial environment, where practical constraints such as latency, computational limitations, and communication reliability can be evaluated under real-world conditions.

Author Contributions: Conceptualization, J.d.l.M., L.M.B. and R.M.; methodology, J.d.l.M.; validation, J.d.l.M., L.M.B. and R.M.; formal analysis, J.d.l.M.; investigation, J.d.l.M.; data curation, J.d.l.M. and L.M.B.; writing—original draft preparation, J.d.l.M.; writing—review and editing, J.d.l.M. and L.M.B.; supervision, L.M.B.; funding acquisition, R.M. All authors have read and agreed to the published version of the manuscript.

Funding: This work was supported by the Spanish Ministry of Science and Innovation (MCIN) grant numbers TED2021-132419B-I00 and PID2022-141978NB-I00; European Project REBBECA (Project ID: 101097224; HORIZON-KDT-JU-2021-2-RIA); and Spanish MCIN/AEI/ 10.13039/501100011033 and the European Union "NextGenerationEU/PRTR" grant number PCI2022-135043-2. This work has also been partially supported by Junta de Comunidades de Castilla-La Mancha/ESF (grant number SBPLY/24/180225/000225).

Data Availability Statement: The raw data supporting the conclusions of this article are available in [19].

Conflicts of Interest: The authors declare no conflict of interest.

References

1. Jiang, W.; Wu, J.; Yang, Y.; Li, X.; Zhu, H. Health Evaluation Techniques Towards Rotating Machinery: A Systematic Literature Review and Implementation Guideline. *Reliab. Eng. Syst. Saf.* **2025**, *260*, 110924. [CrossRef]
2. Elnaggar, M.F.; Flah, A.; Kaana, M.; Mourad, D. A better quality of high-speed software encoder for an aerogenerator-based PMSM machine. *Wind Eng.* **2025**, 0309524X241310141. [CrossRef]
3. Rehman, A.U.; Jiao, W.; Jiang, Y.; Wei, J.; Sohaib, M.; Sun, J.; E, S.; Rehman, K.U.; Chi, Y. Deep learning in industrial machinery: A critical review of bearing fault classification methods. *Appl. Soft Comput.* **2025**, *171*, 112785. [CrossRef]
4. Niu, G.; Dong, X.; Chen, Y. Motor Fault Diagnostics Based on Current Signatures: A Review. *IEEE Trans. Instrum. Meas.* **2023**, *72*, 1–19. [CrossRef]
5. Wright, R.; Fajri, P.; Fu, X.; Asrari, A. Improved Fault Detection Using Shifting Window Data Augmentation of Induction Motor Current Signals. *Energies* **2024**, *17*, 3956. [CrossRef]
6. Wang, X.; Liu, Z.; Dai, M.; Li, W.; Tang, J. Time-Shift Denoising Combined With DWT-Enhanced Condition Domain Adaptation for Motor Bearing Fault Diagnosis via Current Signals. *IEEE Sens. J.* **2024**, *24*, 35019–35035. [CrossRef]
7. De las Morenas, J.; Moya-Fernández, F.; López-Gómez, J.A. The Edge Application of Machine Learning Techniques for Fault Diagnosis in Electrical Machines. *Sensors* **2023**, *23*, 2649. [CrossRef]
8. Konda, Y.R.; Ponnaganti, V.K.; Reddy, P.V.S.; Singh, R.R.; Mercorelli, P.; Gundabattini, E.; Solomon, D.G. Thermal Analysis and Cooling Strategies of High-Efficiency Three-Phase Squirrel-Cage Induction Motors—A Review. *Computation* **2024**, *12*, 6. [CrossRef]
9. Aslan, B.; Balci, S.; Kayabasi, A. Fault diagnosis in thermal images of transformer and asynchronous motor through semantic segmentation and different CNN models. *Appl. Therm. Eng.* **2025**, *265*, 125599. [CrossRef]
10. Siraj, F.M.; Ayon, S.T.K.; Samad, M.A.; Uddin, J.; Choi, K. Few-Shot Lightweight SqueezeNet Architecture for Induction Motor Fault Diagnosis Using Limited Thermal Image Dataset. *IEEE Access* **2024**, *12*, 50986–50997. [CrossRef]
11. Afshar, M.; Heydarzadeh, M.; Akin, B. A Comprehensive Investigation of Fault Signatures and Spectrum Analysis of Vibration Signals in Distributed Bearing Faults. *IEEE Trans. Ind. Appl.* **2025**, *61*, 515–526. [CrossRef]
12. Atif, M.; Azmat, S.; Khan, F.; Albogamy, F.R.; Khan, A. AI-driven thermography-based fault diagnosis in single-phase induction motor. *Results Eng.* **2024**, *24*, 103493. [CrossRef]
13. Daas, A.; Sari, B.; Jia, J.; Rigatos, G. Enhancing induction machine fault detection through machine learning: Time and frequency analysis of vibration signals. *Measurement* **2025**, *242*, 116023. [CrossRef]
14. Gawde, S.; Patil, S.; Kumar, S.; Kamat, P.; Kotecha, K. An explainable predictive maintenance strategy for multi-fault diagnosis of rotating machines using multi-sensor data fusion. *Decis. Anal. J.* **2024**, *10*, 100425. [CrossRef]
15. Memari, M.; Shekaramiz, M.; Masoum, M.A.S.; Seibi, A.C. Data Fusion and Ensemble Learning for Advanced Anomaly Detection Using Multi-Spectral RGB and Thermal Imaging of Small Wind Turbine Blades. *Energies* **2024**, *17*, 673. [CrossRef]
16. Al-Haddad, L.A.; Jaber, A.A.; Hamzah, M.N.; Fayad, M.A. Vibration-current data fusion and gradient boosting classifier for enhanced stator fault diagnosis in three-phase permanent magnet synchronous motors. *Electr. Eng.* **2024**, *106*, 3253–3268. [CrossRef]
17. Soomro, A.A.; Muhammad, M.B.; Mokhtar, A.A.; Md Saad, M.H.; Lashari, N.; Hussain, M.; Sarwar, U.; Palli, A.S. Insights into modern machine learning approaches for bearing fault classification: A systematic literature review. *Results Eng.* **2024**, *23*, 102700. [CrossRef]
18. Abdulkareem, A.; Anyim, T.; Popoola, O.; Abubakar, J.; Ayoade, A. Prediction of induction motor faults using machine learning. *Heliyon* **2025**, *11*, e41493. [CrossRef]
19. Lessmeier, C.; Kimotho, J.K.; Zimmer, D.; Sextro, W. Condition monitoring of bearing damage in electromechanical drive systems by using motor current signals of electric motors: A benchmark data set for data-driven classification. In Proceedings of the PHM society European conference, Bilbao, Spain, 5–8 July 2016; Volume 3. [CrossRef]
20. Orlowska-Kowalska, T.; Wolkiewicz, M.; Pietrzak, P.; Skowron, M.; Ewert, P.; Tarchala, G.; Krzysztofiak, M.; Kowalski, C.T. Fault Diagnosis and Fault-Tolerant Control of PMSM Drives–State of the Art and Future Challenges. *IEEE Access* **2022**, *10*, 59979–60024. [CrossRef]
21. Chen, Z.; Liang, D.; Jia, S.; Yang, S. Model-Based Data Normalization for Data-Driven PMSM Fault Diagnosis. *IEEE Trans. Power Electron.* **2024**, *39*, 11596–11612. [CrossRef]
22. Attaianese, C.; D'Arpino, M.; Monaco, M.D.; Noia, L.P.D. Model-Based Detection and Estimation of DC Offset of Phase Current Sensors for Field Oriented PMSM Drives. *IEEE Trans. Ind. Electron.* **2023**, *70*, 6316–6325. [CrossRef]

23. Abood, S.; Annamalai, A.; Chouikha, M.; Nejress, T. Fault Diagnostics of Synchronous Motor Based on Artificial Intelligence. *Machines* **2025**, *13*, 73. [CrossRef]
24. Luo, P.; Yin, Z.; Zhang, Y.; Bai, C.; Zhang, P.; Liu, J. Increasing Interpretability and Feasibility of Data Driven-Based Unknown Fault Diagnosis in Permanent Magnet Synchronous Motors. In *IEEE Transactions on Energy Conversion*; IEEE: New York, NY, USA, 2024; pp. 1–12. [CrossRef]
25. Siemens Energy & Automation, Inc. *Smart MCCs as a Motor Maintenance Tool*; Siemens Energy & Automation, Inc.: Houston, TX, USA, 2008; A White Paper Issued by SIEMENS.
26. Khawaja, A.U.; Shaf, A.; Thobiani, F.A.; Ali, T.; Irfan, M.; Pirzada, A.R.; Shahkeel, U. Optimizing Bearing Fault Detection: CNN-LSTM with Attentive TabNet for Electric Motor Systems. *CMES-Comput. Model. Eng. Sci.* **2024**, *141*, 2399–2420. [CrossRef]
27. Pacheco-Chérrez, J.; Fortoul-Díaz, J.A.; Cortés-Santacruz, F.; María Aloso-Valerdi, L.; Ibarra-Zarate, D.I. Bearing fault detection with vibration and acoustic signals: Comparison among different machine leaning classification methods. *Eng. Fail. Anal.* **2022**, *139*, 106515. [CrossRef]
28. Deng, L.; Zhao, C.; Yan, X.; Zhang, Y.; Qiu, R. A novel approach for bearing fault diagnosis in complex environments using PSO-CWT and SA-FPN. *Measurement* **2025**, *249*, 117027. [CrossRef]
29. Lv, Y.; Guo, X.; Shirmohammadi, S.; Qian, L.; Gong, Y.; Hu, X. Intelligent Cross-Working Condition Fault Detection and Diagnosis Using Isolation Forest and Adversarial Discriminant Domain Adaptation. *IEEE Trans. Instrum. Meas.* **2024**, *73*, 1–15. [CrossRef]
30. Zhang, X.; Liu, Y.; Gong, C.; Nie, Y.; Rodriguez, J. Electric Motor Bearing Fault Noise Detection via Mel-Spectrum-Based Contrastive Self-Supervised Transformer Model. *IEEE Trans. Ind. Appl.* **2024**, *60*, 8755–8765. [CrossRef]
31. Geraei, H.; Rodriguez, E.A.V.; Majma, E.; Habibi, S.; Al-Ani, D. A Noise Invariant Method for Bearing Fault Detection and Diagnosis Using Adapted Local Binary Pattern (ALBP) and Short-Time Fourier Transform (STFT). *IEEE Access* **2024**, *12*, 107247–107260. [CrossRef]
32. Santer, P.; Reinhard, J.; Schindler, A.; Graichen, K. Detection of localized bearing faults in PMSMs by means of envelope analysis and wavelet packet transform using motor speed and current signals. *Mechatronics* **2025**, *106*, 103294. [CrossRef]
33. Mueller, P.N.; Woelfl, L.; Can, S. Bridging the gap between AI and the industry—A study on bearing fault detection in PMSM-driven systems using CNN and inverter measurement. *Eng. Appl. Artif. Intell.* **2023**, *126*, 106834. [CrossRef]
34. Saleh, M.A.; Ghrayeb, A.; Refaat, S.S.; Abu-Rub, H.; Khatri, S.P.; Kammermann, J. Attention-Enhanced AGRU Framework for Induction Motor Incipient Fault Diagnosis in Electric Vehicles. *IEEE Trans. Instrum. Meas.* **2025**, *74*, 1–17. [CrossRef]
35. Resendiz-Ochoa, E.; Calderon-Uribe, S.; Morales-Hernandez, L.A.; Perez-Ramirez, C.A.; Cruz-Albarran, I.A. Multiple Electromechanical-Failure Detection in Induction Motor Using Thermographic Intensity Profile and Artificial Neural Network. *Machines* **2024**, *12*. [CrossRef]
36. Hoang, D.T.; Kang, H.J. A Motor Current Signal-Based Bearing Fault Diagnosis Using Deep Learning and Information Fusion. *IEEE Trans. Instrum. Meas.* **2020**, *69*, 3325–3333. [CrossRef]
37. Geetha, G.; Geethanjali, P. An efficient method for bearing fault diagnosis. *Syst. Sci. Control Eng.* **2024**, *12*, 2329264. [CrossRef]
38. Luo, Q.; Chen, J.; Zi, Y.; Xie, J. A synchronization-induced cross-modal contrastive learning strategy for fault diagnosis of electromechanical systems under semi-supervised learning with current signal. *Expert Syst. Appl.* **2024**, *249*, 123801. [CrossRef]
39. Li, H.; Wang, D. Multilevel feature fusion of multi-domain vibration signals for bearing fault diagnosis. *Signal Image Video Process.* **2024**, *18*, 99–108. [CrossRef]
40. Nishat Toma, R.; Kim, J.M. Bearing Fault Classification of Induction Motors Using Discrete Wavelet Transform and Ensemble Machine Learning Algorithms. *Appl. Sci.* **2020**, *10*, 5251. [CrossRef]
41. Toma, R.N.; Prosvirin, A.E.; Kim, J.M. Bearing Fault Diagnosis of Induction Motors Using a Genetic Algorithm and Machine Learning Classifiers. *Sensors* **2020**, *20*, 1884. [CrossRef]
42. El Hachemi Benbouzid, M. A review of induction motors signature analysis as a medium for faults detection. *IEEE Trans. Ind. Electron.* **2000**, *47*, 984–993. [CrossRef]
43. Zhang, S.; Wang, B.; Kanemaru, M.; Lin, C.; Liu, D.; Miyoshi, M.; Teo, K.H.; Habetler, T.G. Model-Based Analysis and Quantification of Bearing Faults in Induction Machines. *IEEE Trans. Ind. Appl.* **2020**, *56*, 2158–2170. [CrossRef]
44. Zhang, B.; Li, H.; Kong, W.; Fu, M.; Ma, J. Early-Stage Fault Diagnosis of Motor Bearing Based on Kurtosis Weighting and Fusion of Current–Vibration Signals. *Sensors* **2024**, *24*, 3373. [CrossRef] [PubMed]
45. Schiltz, R.L. Forcing frequency identification of rolling element bearings. *Sound Vib.* **1990**, *24*, 16–19.
46. Song, X.; Hu, J.; Zhu, H.; Zhang, J. A bearing outer raceway fault detection method in induction motors based on instantaneous frequency of the stator current. *IEEJ Trans. Electr. Electron. Eng.* **2018**, *13*, 510–516. [CrossRef]
47. Classification Based on Decision Tree Algorithm for Machine Learning. *J. Appl. Sci. Technol. Trends* **2021**, *2*, 20–28. [CrossRef]
48. Park, J.; Kang, D. Artificial Intelligence and Smart Technologies in Safety Management: A Comprehensive Analysis Across Multiple Industries. *Appl. Sci.* **2024**, *14*, 11934. [CrossRef]

49. Longo, L.; Brcic, M.; Cabitza, F.; Choi, J.; Confalonieri, R.; Ser, J.D.; Guidotti, R.; Hayashi, Y.; Herrera, F.; Holzinger, A.; et al. Explainable Artificial Intelligence (XAI) 2.0: A manifesto of open challenges and interdisciplinary research directions. *Inf. Fusion* **2024**, *106*, 102301. [CrossRef]
50. Breiman, L. Random Forests. *Mach. Learn.* **2001**, *45*, 5–32. [CrossRef]
51. Chen, T.; Guestrin, C. XGBoost: A Scalable Tree Boosting System. In Proceedings of the 22nd ACM SIGKDD International Conference on Knowledge Discovery and Data Mining, New York, NY, USA, 13–17 August 2016; KDD '16; pp. 785–794. [CrossRef]
52. Ke, G.; Meng, Q.; Finley, T.; Wang, T.; Chen, W.; Ma, W.; Ye, Q.; Liu, T.Y. LightGBM: A Highly Efficient Gradient Boosting Decision Tree. In *Advances in Neural Information Processing Systems*; Guyon, I., Luxburg, U.V., Bengio, S., Wallach, H., Fergus, R., Vishwanathan, S., Garnett, R., Eds.; Curran Associates, Inc.: Red Hook, NY, USA, 2017; Volume 30.
53. Prokhorenkova, L.; Gusev, G.; Vorobev, A.; Dorogush, A.V.; Gulin, A. CatBoost: Unbiased boosting with categorical features. In *Advances in Neural Information Processing Systems*; Bengio, S., Wallach, H., Larochelle, H., Grauman, K., Cesa-Bianchi, N., Garnett, R., Eds.; Curran Associates, Inc.: Red Hook, NY, USA, 2018; Volume 31.
54. Pinkus, A. Approximation theory of the MLP model in neural networks. *Acta Numer.* **1999**, *8*, 143–195. [CrossRef]
55. Ali, Y.A.; Awwad, E.M.; Al-Razgan, M.; Maarouf, A. Hyperparameter Search for Machine Learning Algorithms for Optimizing the Computational Complexity. *Processes* **2023**, *11*, 349. [CrossRef]
56. Dunbar, O.R.A.; Nelsen, N.H.; Mutic, M. Hyperparameter optimization for randomized algorithms: A case study on random features. *Stat. Comput.* **2025**, *35*, 56. [CrossRef]
57. Di Fiore, F.; Nardelli, M.; Mainini, L. Active Learning and Bayesian Optimization: A Unified Perspective to Learn with a Goal. *Arch. Comput. Methods Eng.* **2024**, *31*, 2985–3013. [CrossRef]

Disclaimer/Publisher's Note: The statements, opinions and data contained in all publications are solely those of the individual author(s) and contributor(s) and not of MDPI and/or the editor(s). MDPI and/or the editor(s) disclaim responsibility for any injury to people or property resulting from any ideas, methods, instructions or products referred to in the content.